

## FULL EVOLUTION OF THE 6 AND 20 CENTIMETER RADIO EMISSION FROM SN 1980K

KURT W. WEILER AND SCHUYLER D. VAN DYK<sup>1</sup>

Center for Advanced Space Sensing, Naval Research Laboratory, Code 4215, Washington, DC 20375-5000

NINO PANAGIA<sup>2,3</sup>

Space Telescope Science Institute, 3700 San Martin Drive, Baltimore, MD 21218

AND

RICHARD A. SRAMEK

National Radio Astronomy Observatory, P.O. Box O, Socorro, NM 87801

Received 1991 December 2; accepted 1992 April 13

### ABSTRACT

First detected at 6 cm in 1980 November, only 1 month after optical maximum, and several months later at 20 cm in 1981 March, SN 1980K has now dropped below reasonable monitoring limits of the VLA at these two frequencies. It thus represents the first Type II radio supernova to have been well-studied at centimeter wavelengths from “turn-on” to “turn-off.” It also represents one of the few radio supernovae to have such an extensive, decade-long, multiple-frequency data set.

We present new observations of SN 1980K made with the VLA at 20 and 6 cm from 1984 November through 1990 December. Unless the radio emission strengthens again in the future, this completes our monitoring of the supernova at these wavelengths.

The study of these “complete” light curves shows that the “minishell” model of Chevalier still provides the best representation of the data at both wavelengths. The similarities between the behavior of the radio emission from SN 1980K and SN 1979C argue that these two objects represent a distinct class of radio supernovae which is distinguishable from the radio emission from Type Ib supernovae, such as SN 1983N and SN 1984L, or the radio emission from the presumed Type II supernova SN 1986J. The implication is that there exist several classes of radio-emitting supernovae whose differing radio properties probably arise from different mass-loss rates and therefore different zero-age main-sequence masses of progenitor stars.

*Subject headings:* radio continuum: stars — supernovae: individual (SN 1980K)

### 1. INTRODUCTION

In a recent paper (Weiler et al. 1991) we presented the results of long term monitoring of the radio emission from the Type II supernova SN 1979C. For the 10 yr of available observations on the supernova (SN), we found that it behaves in a regular manner and shows the properties of: (1) nonthermal emission with high brightness temperature; (2) light curve “turn-on” at shorter radio wavelengths first and longer wavelengths later; (3) an initial rapid increase of flux density with time at each wavelength, with a power-law decline after maximum is reached; and (4) a sharp initial decrease in spectral index between two wavelengths, as the longer wavelength emission goes from being optically thick to thin, with the spectral index value,  $\alpha$ , asymptotically approaching an optically thin, non-thermal, constant negative value. We present here a second radio SN (RSN), SN 1980K, which, over a comparable 10 yr monitoring period, shows basic properties identical to those of SN 1979C.

SN 1980K [ $\alpha(1950.0) = 20^{\text{h}}34^{\text{m}}26^{\text{s}}.68 \pm 0^{\text{s}}.01$ ;  $\delta(1950.0) = +59^{\circ}55'56''.5 \pm 0''.2$ ] in NGC 6946 was discovered in 1980 October by Wild (1980), and an initial unsuccessful attempt was made in early 1980 November to detect it at 6 cm with the

Very Large Array (VLA).<sup>4</sup> At 35 days after optical maximum (which is estimated to have occurred on 1980 October 30), the SN was detected at 6 cm, and we have been regularly monitoring it with the VLA at wavelengths 20, 6, and, occasionally, 2 cm ever since. The results of observations from 1980 November through 1984 August are contained in Weiler et al. (1986). We present here subsequent monitoring results at 20 and 6 cm (the SN was at the less than 0.2 mJy level at 2 cm in 1984 March and thus below reasonable VLA detection limits) from 1984 November through 1990 December. Since SN 1980K is now below reasonable monitoring limits with the VLA at both wavelengths, no further regular observations are planned. (Occasional measurements, to check that the source has not rebrightened, will, of course, be carried out in the future.) These light curves thus define the “full evolution” of radio emission from the Type II SN 1980K during a period of  $\sim 10$  yr.

### 2. OBSERVATIONS

The new observations of SN 1980K were made with the VLA at 20 cm (1.490 GHz) and 6 cm (4.860 GHz) from 1984 November through 1990 December at roughly a quarterly rate. Since monitoring of an evolving radio source requires measurement at frequent intervals, we were not able to request the VLA configuration and consequently have measurements at all array sizes. Along with each observation of the source, a short

<sup>1</sup> Naval Research Lab/National Research Council Cooperative Research Associate.

<sup>2</sup> Affiliated with the Astrophysics Division, Space Science Department of ESA.

<sup>3</sup> Also University of Catania, Italy.

<sup>4</sup> The VLA is operated by the National Radio Astronomy Observatory of Associated Universities, Inc., under a cooperative agreement with the National Science Foundation.

TABLE 1  
CALIBRATION SOURCES

Source Name (1)	Calibrator Type (2)	$\alpha_{1950.0}$ (3)	$\delta_{1950.0}$ (4)	$S_{20}$ (Jy) (5)	$S_6$ (Jy) (6)
3C 48 .....	Primary	Not used	Not used	14.60	5.60
2021+614 <sup>a</sup> .....	Secondary	20 <sup>h</sup> 21 <sup>m</sup> 13 <sup>s</sup> .297	+61°27'18".12	...	...

<sup>a</sup> See Table 2 for flux densities.

observation of a “secondary,” possibly variable, calibrator, 2021+614, was made at each frequency. To establish an absolute flux density scale, most observing sessions also included an observation of a “primary,” presumed constant, calibrator 3C 48.

2.1. Calibration

The VLA is described in a number of publications (e.g., Thompson et al. 1980; Hjellming & Bignell 1982; Napier, Thompson, & Ekers 1983); the general procedures for RSN observations, with analysis of the possible sources of error, are discussed in Weiler et al. (1986). The “primary” calibrator employed here, 3C 48, was assumed to be constant in flux density with time and to have the flux densities at 20 and 6 cm given in Table 1.

The “secondary” calibrator, 2021+614, was used as the phase (position) and amplitude (flux density) reference for the observations of SN 1980K. Its assumed position (epoch 1950.0) is given in Table 1, and its flux density values, measured against 3C 48, at 20 cm ( $S_{20}$ ) and 6 cm ( $S_6$ ) are presented for each observing date in Table 2.

2.2. Data Reduction

After the data were initially calibrated using standard software packages on the DEC-10 and Convex computers at the

VLA, the data were “exported” to the Naval Research Laboratory for analysis with AIPS on the local VAX 11/785 and Alliant VFX/40 computers. Most data sets were individually hand-edited, mapped, CLEANed, inspected, and then independently measured in both IF channels for each observing band. The flux density values from the two IF channels were then averaged to obtain a final measurement of the flux density in each band at each epoch. Observations after 1989 December were mapped by combining both IF channels into a single map before measurement.

2.3. Errors

One estimate for the flux density measurement error is the rms “map” error,  $\sigma_0$ , which measures the contribution of small, unresolved fluctuations in the background emission and random map fluctuations due to receiver noise. For strong sources, this can be considered only a lower limit to the total error. Comparison of the two IF channel flux density solutions is clearly too small of a sample to provide meaningful statistics; also, the two IF channels do not provide truly independent solutions for a number of types of instrumental errors. Therefore, errors for the measurements in this paper include a basic 5% error to account for the normal inaccuracy of VLA flux density measurements and any absolute scale error for the primary calibrator, 3C 48. The final errors,  $\sigma_f$ , listed in Table 3, are taken as

$$\sigma_f^2 \equiv (0.05S_0)^2 + \sigma_0^2, \tag{1}$$

where  $S_0$  is the observed flux density for SN 1980K and  $\sigma_0$  is the observed rms map error measured outside of any obvious regions of emission.

One instrumental problem which had to be taken into account might be called the “configuration” error. At long wavelengths and short baselines (i.e., low resolving power), the contribution of the flux density per beam area from the particularly bright and structured nuclear and disk emission of the parent galaxy, NGC 6946, was severe relative to the weak SN emission. In the compact C- and D-configurations of the VLA the confusion and resulting large errors in the 20 cm maps made flux density measurements futile, and even measurements at 6 cm in D-configuration at later epochs, when SN 1980K had considerably weakened, were useless. Therefore, most of the flux density values listed in Table 3 at 20 and 6 cm in C- and D-configurations are (3  $\sigma$ ) upper limits.

3. RESULTS

Since the previous publication of SN 1980K data in Weiler et al. (1986), we have added 10 new measurements (and four upper limits) at 20 cm and 19 new measurements (and two upper limits) at 6 cm. We present these in Table 3. Column (1) is the date of observation; column (2) is the time, in days, since

TABLE 2  
MEASURED FLUX DENSITY VALUES FOR THE  
SECONDARY CALIBRATOR 2021+614<sup>a</sup>

Observation Date (1)	$S_{20}$ (Jy) (2)	$S_6$ (Jy) (3)
1984 Nov 21 .....	2.250	2.410
1985 Mar 21 .....	2.190	2.360
1985 Jul 5 .....	2.190	2.416
1985 Sep 23 .....	2.138	2.343
1985 Dec 22 .....	...	2.417
1986 Mar 27 .....	2.218	2.424
1986 Jun 11 .....	2.234	2.507
1986 Dec 23 .....	...	2.490
1987 Mar 16 .....	...	3.117
1987 Jun 25 .....	2.190	2.550
1987 Sep 9 .....	2.165	2.685
1987 Dec 20 .....	1.855	2.735
1988 Sep 16 .....	2.180	2.610
1988 Dec 23 .....	2.200	2.610
1989 Apr 24 .....	2.165	2.645
1989 Jul 23 .....	2.067	2.656
1989 Dec 23 .....	...	2.647
1990 Feb 15 .....	...	2.849
1990 May 29 .....	...	2.796
1990 Aug 27 .....	...	2.696
1990 Dec 9 .....	2.746	2.679

<sup>a</sup> Independently calibrated using 3C 48.

TABLE 3  
NEW FLUX DENSITY AND SPECTRAL INDEX MEASUREMENTS FOR SN 1980K<sup>a</sup>

OBSERVATION DATE (1)	TIME SINCE OPTICAL MAXIMUM <sup>b</sup> (days) (2)	VLA CONFIGURATION (3)	FLUX DENSITY				SPECTRAL INDEX ( $S \propto \nu^{\alpha}$ )	
			$S_{20}$ (mJy) (4)	$\sigma_{20}$ (mJy) (5)	$S_6$ (mJy) (6)	$\sigma_6$ (mJy) (7)	$\alpha_{6}^{20}$ (8)	$\sigma_{\alpha_{6}^{20}}$ (9)
1980 Oct 30 .....	$\equiv 0$							
1984 Nov 21 .....	1483	A	1.21	0.17	0.57	0.10	-0.64	0.20
1985 Mar 21 .....	1603	A/B	1.14	0.22	0.51	0.08	-0.68	0.21
1985 Jul 5 .....	1709	B/C	0.95	0.21	0.66	0.10	-0.31	0.22
1985 Sep 23 .....	1789	C	<0.83 <sup>c</sup>	...	0.55	0.08	...	...
1985 Dec 22 .....	1879	D	...	...	0.53	0.08	...	...
1986 Mar 27 .....	1974	A	1.16	0.13	0.37	0.07	-0.97	0.19
1986 Jun 11 .....	2050	A/B	0.79	0.18	0.43	0.10	-0.51	0.28
1986 Dec 23 .....	2245	C	...	...	0.42	0.15	...	...
1987 Mar 16 .....	2328	D	...	...	0.29	0.12	...	...
1987 Jun 25 .....	2429	A	0.50	0.14	0.33	0.06	-0.35	0.29
1987 Sep 9 .....	2505	A	0.60	0.16	0.26	0.08	-0.71	0.35
1987 Dec 20 .....	2607	B	0.75	0.23	0.37	0.11	-0.60	0.37
1988 Sep 16 .....	2878	D	...	...	0.44	0.13	...	...
1988 Dec 23 .....	2976	A	0.44	0.11	0.28	0.06	-0.38	0.28
1989 Apr 24 .....	3098	B	0.59	0.17	0.26	0.06	-0.69	0.32
1989 Jul 23 .....	3188	C	<1.20 <sup>c</sup>	...	0.34	0.08	...	...
1989 Dec 23 .....	3341	D	...	...	<0.42 <sup>c</sup>	...	...	...
1990 Feb 15 .....	3395	A	...	...	0.24	0.05	...	...
1990 May 29 .....	3498	A	...	...	0.25	0.07	...	...
1990 Aug 27 .....	3588	B	...	...	<0.15 <sup>c</sup>	...	...	...
1990 Dec 9 .....	3692	C	<1.26 <sup>c</sup>	...	0.28	0.09	...	...

<sup>a</sup> For previous measurements, see Weiler et al. 1986.

<sup>b</sup> The date of the explosion is taken to be 1980 October 1, 29 days before optical maximum (see Weiler et al. 1986).

<sup>c</sup> 3  $\sigma$  upper limit.

optical maximum (the date of explosion is taken by Weiler et al. 1986 to have been 29 days before optical maximum, or 1980 October 1); column (3) gives the VLA configuration in which the SN was observed; columns (4) and (6) give the measured flux densities at 20 cm ( $S_{20}$ ) and 6 cm ( $S_6$ ), respectively; and columns (5) and (7) give the error estimates for these measurements. Table 3 also contains determinations of the spectral index,  $\alpha$ , from our data ( $S \propto \nu^{\alpha}$ ), with column (8) listing the spectral index,  $\alpha_{6}^{20}$ , between 20 and 6 cm, and column (9), its error,  $\sigma_{\alpha_{6}^{20}}$ .

In Figure 1 we plot the time evolution of the flux density of SN 1980K in both radio bands, including the new results together with the earlier measurements from Weiler et al. (1986). The solid lines are the "best-fit" model light curves discussed below. In Figure 2 we show the change in spectral index between 20 and 6 cm with time over the decade since explosion. One can see from Figure 2 that the spectral index change is very similar to that found by Weiler et al. (1986), with  $\alpha_{6}^{20}$  asymptotically approaching a value of  $\sim -0.5$ . The solid curve shown in Figure 2 is not an independent fit, but is calculated from the model light curves shown in Figure 1.

#### 4. DISCUSSION

Previous work on radio supernovae (RSNs) has shown that we have a reasonable understanding of the behavior and mechanisms involved in generating the observed radio emission.

##### 4.1. Radio Light Curves

Following Weiler et al. (1986), we assume that:

a) The radio emission is due to the nonthermal synchrotron process with optically thin spectral index,  $\alpha$ ;

b) The absorption or optical depth,  $\tau$ , is purely of a thermal, free-free nature in an ionized medium (frequency dependence  $\nu^{-2.1}$ ) external to the emitting region with a radial density dependence  $\rho \propto r^{-2}$  from a red supergiant wind of constant speed; and,

c) The observed flux density,  $S$ , and the optical depth,  $\tau$ , can be well described as functions of SN age,  $t - t_0$ , to the powers  $\beta$  and  $\delta$ , respectively, after an explosion epoch  $t_0$ . This formulation can be written as

$$S(\text{mJy}) = K_1 \left( \frac{\nu}{5 \text{ GHz}} \right)^{\alpha} \left( \frac{t - t_0}{1 \text{ day}} \right)^{\beta} e^{-\tau}, \quad (2)$$

where

$$\tau = K_2 \left( \frac{\nu}{5 \text{ GHz}} \right)^{-2.1} \left( \frac{t - t_0}{1 \text{ day}} \right)^{\delta}. \quad (3)$$

The factors  $K_1$  and  $K_2$  above are scaling parameters for the units of choice (mJy, GHz, and days) and formally correspond to the flux density and optical depth, respectively, at 5 GHz, 1 day after the explosion.

Mixed, internal absorbing and emitting processes could not cause the initial radio light curve to rise as quickly as observed (cf. Marshner & Brown 1978) and, if the location of the absorbing material is external, only a thermal process is possible. The two nonthermal processes for absorption, the Razin-Tsytoich effect and synchrotron self-absorption, require densities that are impossibly high for regions surrounding a SN (cf. Marscher & Brown 1978; Chevalier 1982a, b; Bandiera, Pacini, & Salvati 1984). The single known RSN exception to this purely external, thermal

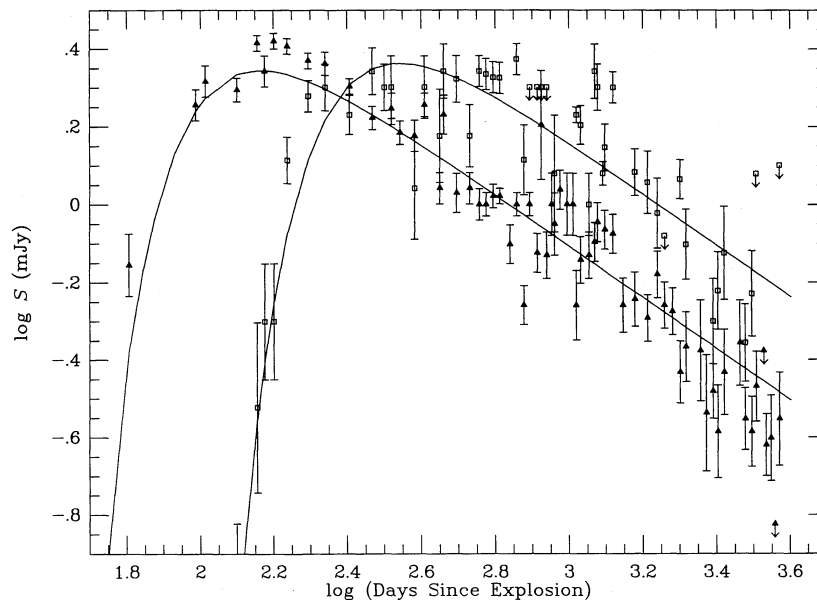


FIG. 1.—Radio “light curves” for SN 1980K in NGC 6946. The wavelengths 20 cm (*open squares*) and 6 cm (*filled triangles*), are shown together. The data represent more than 10 yr of observations for this object, including new observations presented in this paper and previous measurements from Weiler et al. (1986). The age of the SN is measured in days from the estimated date of explosion on 1980 October 1 (29 days before optical maximum). The solid lines represent the best-fit light curves of the form  $S(\text{mJy}) = K_1 [\nu/(5 \text{ GHz})]^\alpha [(t - t_0)/(1 \text{ day})]^\beta e^{-\tau}$ , where  $\tau = K_2 [\nu/(5 \text{ GHz})]^{-2.1} [(t - t_0)/(1 \text{ day})]^\delta$ , and  $\delta \equiv \alpha - \beta - 3$ .

absorption behavior is SN 1986J, which shows an entirely different type of radio light curve and appears to require mixed, internal, nonthermal emitting/thermal absorbing gas. SN 1986J is described in detail elsewhere (Weiler, Panagia, & Sramek 1990).

The full available data set at 20 and 6 cm, including the values from Weiler et al. (1986), was then used to solve for the four free parameters,  $K_1$ ,  $K_2$ ,  $\alpha$ , and  $\beta$ , in equations (2) and (3). Following Weiler et al. (1986) we have defined the date of explosion,  $t_0$ , as 29 days before optical maximum (or 1980 October 1),<sup>5</sup> and because of the success of the Chevalier model (Chevalier 1981a, b; 1984a, b) for RSN emission (see also Weiler et al. 1986, 1990, 1991; and Note [d] to Table 4), we defined  $\delta$  to be (Chevalier 1984b).

$$\delta \equiv \alpha - \beta - 3. \quad (4)$$

The “best” fit was obtained by using a minimum reduced  $\chi^2$  procedure to identify the best value and range of values for each of the parameters, which are listed in Table 4. A minimum measurement error of 17% was required to bring  $\chi_{\text{red}}^2$  from  $\sim 2.7$  down to  $\sim 1.0$  per degree of freedom. This need to increase the data errors beyond the level of  $\sim 5\%$  for points near flux density maximum in order to obtain a  $\chi_{\text{red}}^2 \sim 1$  likely results from the fact that the model of equations (2) and (3) is not sufficiently complex to fully describe any short-term fluctuations in the RSN radio light curves (cf. Weiler et al. 1991). The range of uncertainty listed for each parameter in Table 4 is the amount that a parameter must deviate from the best-fit value in order to increase  $\chi_{\text{red}}^2$  from  $\sim 1$  to  $\sim 5$  (Abramowitz & Stegun 1965). This is appropriate for a four-parameter fit and

<sup>5</sup> By varying  $t_0$  and examining  $\chi_{\text{red}}^2$ , we find that  $t_0 = 1980$  September 25, 35 days before optical maximum, actually produces a slightly improved fit to the data ( $\chi_{\text{red}}^2[t_0 = 35 \text{ days}] \simeq 2.66$ , while  $\chi_{\text{red}}^2[t_0 = 29 \text{ days}] \simeq 2.70$ ). However, since this variation in the initial epoch is quite small and within the range for  $t_0$  given in Weiler et al. (1986), for the sake of consistency, we maintain  $t_0 = 1980$  October 1.

determines the 67% probability intervals within which the true values lie; i.e., the error range analogous to the  $1 \sigma$  uncertainty for a single parameter fit. The model curves calculated with equations (2) and (3) for the parameter values of Table 4 are shown as the solid lines in Figure 1, and, as can be seen, provide a good fit to the data points. In Figure 2, the spectral index evolution is very regular and also well-described by equations (2) and (3) with the parameters from Table 4.

Examination of Figures 1 and 2 shows that the model curves, even for such a simple model, describe the available data at both frequencies rather well in gross terms. The parameters listed in Table 4, in fact, generally agree with those determined from the more limited data set available to Weiler et al.

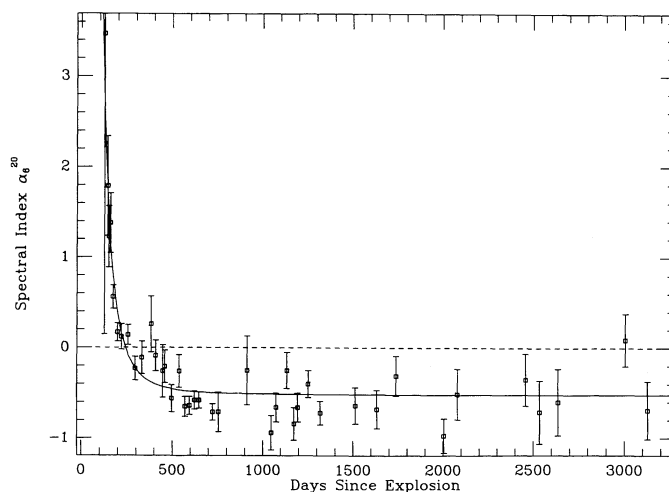


FIG. 2.—Spectral index  $\alpha$  ( $S \propto \nu^{+\alpha}$ ) evolution for SN 1980K between 20 cm and 6 cm, plotted as a function of time, in days, since the estimated explosion date of 1980 October 1 (29 days before optical maximum). The solid line is calculated from the best-fit theoretical “light curves” shown in Fig. 1. The dashed line shows  $\alpha = 0$ .

TABLE 4  
FITTING PARAMETERS FOR SN 1980K<sup>a,b</sup>

Parameter (1)	Value (2)	Deviation Range <sup>c</sup> (3)
$K_1$ .....	74	40–103
$\alpha$ .....	–0.52	–(0.19–0.68)
$\beta$ .....	–0.66	–(0.62–0.74)
$K_2$ .....	$3.37 \times 10^5$	$(1.2–32.0) \times 10^5$
$\delta (\equiv \alpha - \beta - 3)^d$ .....	–2.86	–(2.46–3.07)
$t_0^e$ .....	$\equiv$ 1980 Oct 1	1980 Jul 2–1980 Oct 29
$\dot{M}^f (M_\odot \text{ yr}^{-1})$ .....	$2.6 \times 10^{-5}$	

<sup>a</sup> The radio light curves are assumed to fit a curve of the form:  $S(\text{mJy}) = K_1 [v/5 \text{ GHz}]^\tau [(t - t_0)/(1 \text{ day})]^\delta e^{-\tau}$ , where  $\tau = K_2 [v/5 \text{ GHz}]^{-2.1} [(t - t_0)/(1 \text{ day})]^\delta$ . From Chevalier (1984b),  $\delta \equiv \alpha - \beta - 3$  is assumed.

<sup>b</sup> With a minimum measurement error of 17% for the measured flux densities to account for the fact that no simple model can completely describe such a complicated phenomenon, these parameters yield a  $\chi^2_{\text{red}} \approx 1.0$ .

<sup>c</sup> The Deviation Range is the range in which there is a  $\sim 67\%$  probability that the true value lies. This is equivalent to a  $1 \sigma$  range for a one-parameter solution.

<sup>d</sup> If  $\delta$  is allowed to vary in the fitting procedure, the minimum  $\chi^2_{\text{red}} \approx 1.0$  remains for the range in  $\delta$  from  $-2.92$  to  $-2.75$ . Since this range includes the value of  $\delta$  assuming the Chevalier model ( $\delta \equiv \alpha - \beta - 3$ ), our acceptance of the model appears supported.

<sup>e</sup> The date of the explosion is taken to be 1980 October 1, following Weiler et al. 1986.

<sup>f</sup> The mass-loss rate is estimated from eq. (16) in Weiler et al. 1986.

(1986) to within the fitting uncertainties (Weiler et al. give  $K_1 = 73 \pm 12$ ,  $\alpha = -0.50 \pm 0.06$ ,  $\beta = -0.65 \pm 0.10$ , and  $K_2 = [2.8 \pm 0.3] \times 10^5$ ).

The radio emission of SN 1980K is clearly evolving in a regular manner. There have been no extreme brightenings or fadings caused by large density fluctuations in the red supergiant wind or by approaching the wind's outer boundary. The wind boundary, at which Weiler et al. (1986) predicted that radio emission should sharply cut off, has clearly not yet been reached.

#### 4.2. Models

Two models, the “minishell” (shock acceleration of the relativistic particles generating the nonthermal radio emission occurs in a region external to the SN photosphere, e.g., the Cas A SN remnant) and the “miniplerion” (“pulsar” generation of the radio-emitting relativistic particles and magnetic fields occurs at the center of the SN, e.g., the Crab Nebula SN remnant), have been suggested to provide the mechanism for the acceleration of the relativistic particles generating the non-thermal emission from RSNs (see Weiler et al. 1986). Weiler et al. (1986) showed that for the measurements through 1984 for SN 1980K the minishell model provided a significantly better fit to the data than did the miniplerion model. In the present paper, through an analysis similar to that used by Weiler et al. (1991) for SN 1979C, including the additional data for SN 1980K from 1985 to 1990, we find that the minishell model still represents the best description for the radio emission and the miniplerion case can be ruled out.

#### 4.3. Short-Period Light Curve Deviations

Although the very similar RSN SN 1979C appears to have significant short-period deviations from the fitted light curves (see Weiler et al. 1991), and examination of Figure 1 shows SN

1980K to deviate at times from the smooth curves described by equations (2) and (3) and Table 4, the source is too weak and the errors in the flux density measurements are too large to establish this with certainty. Plots of the flux density deviations from the fitted curves at 20 and 6 cm and power spectrum analysis of those deviations are unconvincing.

#### 4.4. Mass Loss from the Progenitor

An estimate of the mass-loss rate for the assumed pre-SN red supergiant progenitor star can be made using the simplified formula of equation (16) in Weiler et al. (1986). Adopting a wind velocity,  $w \sim 10 \text{ km s}^{-1}$ , an optical expansion velocity of the SN ejecta,  $v_i \approx 1.3 \times 10^4 \text{ km s}^{-1}$ , and an electron temperature in the wind,  $T \sim 3 \times 10^4 \text{ K}$  (Lundqvist & Fransson 1988), the mass loss is estimated to be  $\dot{M} \approx 2.6 \times 10^{-5} M_\odot \text{ yr}^{-1}$ . Assuming that the wind velocity,  $w$ , during this mass loss was constant, the duration of this mass-loss epoch,  $\Delta t_M$ , is the ratio of the radius of the wind-blown circumstellar shell,  $R_{\text{shell}}$ , to the velocity  $w$ . From the known time (10.2 yr) of interaction of the rapidly moving SN ejecta ( $\sim 1.3 \times 10^4 \text{ km s}^{-1}$ ) with the shell material, which gives rise to the observed radio emission, we can estimate  $R_{\text{shell}} \gtrsim 4.2 \times 10^{17} \text{ cm}$ . If the shell was established by a red supergiant wind moving at  $\sim 10 \text{ km s}^{-1}$ , a duration of high mass loss of  $\Delta t_M \gtrsim 1.3 \times 10^4 \text{ yr}$  must hold. Thus, we can also place a lower limit on the amount of mass lost from the progenitor, assumed to occur during the red supergiant phase, of  $\Delta M \gtrsim 0.34 M_\odot$ .

The stellar evolution models of Maeder & Meynet (1988) show that a  $7 M_\odot$  zero-age main-sequence (ZAMS) star experiences a mass loss of  $\sim 0.32 M_\odot$  by the end of C-core burning. Therefore we can place a lower limit on the ZAMS mass of the progenitor of SN 1980K to be  $\gtrsim 7 M_\odot$ . Although this is somewhat less than what is generally thought to be the lower mass limit ( $\sim 8 M_\odot$ ) for Type II SN progenitors (cf. Woosley & Weaver 1986), it is not inconsistent with the 4–5  $M_\odot$  upper limit for main-sequence white dwarf progenitors found in open clusters (e.g., Reimers & Koester 1989) or the critical mass necessary for nondegenerate C-core burning (e.g., Castellani et al. 1985). With an upper mass limit of  $18 M_\odot$  placed on the progenitor of SN 1980K by Thompson (1982), we can now constrain the progenitor mass at  $7 M_\odot \lesssim M \lesssim 18 M_\odot$ . We conclude that the progenitor of SN 1980K was likely to have been less massive than the progenitor of SN 1979C ( $M \gtrsim 13 M_\odot$ ; cf. Weiler et al. 1991), whose 10 yr radio evolution SN 1980K so closely resembles, confirming that the progenitors of Type II SNe fall in a broad range of ZAMS masses.

#### 5. COMPARISON WITH OTHER RSNs

Weiler et al. (1986), even with their more limited data sets, were able to distinguish two categories of radio-emitting SNe, subclass Type Ib such as SN 1983N (called Type I<sub>SL</sub>, for Type I subluminal, by them) and Type II such as SN 1979C. Since that time, Weiler et al. (1990) have established a third category of RSN in the Type II SN 1986J. Each of these classes appears distinguishable in terms of spectral index, radio turn-on rate, decline rate after maximum at each frequency, and the ratio of internal to external absorption. While we shall reserve detailed discussion of the classification of RSNs to another paper, it is clear that SN 1980K much more closely resembles the Type II SN 1979C in the details of its radio emission than either of the two other known categories. Thus, SN 1980K appears to be a second, albeit lower mass-progenitor star, example of the

physical process leading to Type II SN explosions such as occurred in the case of SN 1979C.

#### 6. CONCLUSIONS

Analysis of the radio emission from the Type II RSN SN 1980K at 20 and 6 cm leads to the following conclusions.

1. The emission from SN 1980K is continuing its regular decline in flux density with time.
2. The light curves, including the most recent data, are still consistent with the model for nonthermal emission with external, thermal absorption.
3. The best-fit parameters differ only slightly, and are within the statistical errors, from the values obtained by Weiler et al. (1986), indicating that the model is still accurate 10 yr after explosion.
4. The earlier preference for the minishell model to describe

the nonthermal emission for SN 1980K is still supported by the new data.

5. The red supergiant progenitor for SN 1980K maintained a mass-loss rate of greater than  $10^{-5} M_{\odot} \text{ yr}^{-1}$  for at least  $1 \times 10^4$  yr before explosion.

6. A lower limit of  $\gtrsim 0.34 M_{\odot}$  can be accounted for as having been lost from the progenitor in the pre-SN stellar wind, allowing us to place a lower limit on the zero-age main-sequence mass of the progenitor star of  $\gtrsim 7 M_{\odot}$ .

7. SN 1980K appears to belong to the distinguishable class of RSNs which are similar in radio properties to SN 1979C.

We wish to thank Jennifer L. Discenna for her assistance at the Naval Research Lab in the production and analysis of the radio maps of SN 1980K. We also thank the referee, Stephen Reynolds, for very helpful comments regarding this paper.

#### REFERENCES

- Abramowitz, M., & Stegun, I. A. 1965, *Handbook of Mathematical Functions* (New York: Dover), 980
- Bandiera, R., Pacini, F., & Salvati, M. 1984, *ApJ*, 285, 134
- Castellani, V., Chieffi, A., Pulone, L., & Tornambe, A. 1985, *ApJ*, 294, L31
- Chevalier, R. A. 1981a, *ApJ*, 251, 259
- . 1981b, *ApJ*, 246, 267
- . 1982a, *ApJ*, 259, 302
- . 1982b, *ApJ*, 259, L85
- . 1984a, *Ann. NY Acad. Sci.*, 422, 215
- . 1984b, *ApJ*, 285, L63
- Hjellming, R. M., & Bignell, R. C. 1982, *Science*, 216, 1279
- Lundqvist, P., & Fransson, C. 1988, *A&A*, 192, 221
- Maeder, A., & Meynet, G. 1988, *A&AS*, 76, 411
- Marscher, A. P., & Brown, R. L. 1978, *ApJ*, 220, 474
- Napier, P. J., Thompson, A. R., & Ekers, R. D. 1983, *Proc. IEEE*, 71, 1295
- Reimers, D., & Koester, D. 1989, *A&A*, 218, 118
- Thompson, A. R., Clark, B. G., Wade, C. M., & Napier, P. J. 1980, *ApJS*, 44, 151
- Thompson, L. A. 1982, *ApJ*, 257, L63
- Weiler, K. W., Panagia, N., & Sramek, R. A. 1990, *ApJ*, 364, 611
- Weiler, K. W., Sramek, R. A., Panagia, N., van der Hulst, J. M., & Salvati, M. 1986, *ApJ*, 301, 790
- Weiler, K. W., Van Dyk, S. D., Panagia, N., Sramek, R. A., & Discenna, J. L. 1991, *ApJ*, 380, 161
- Wild, P. 1980, *IAU Circ.*, No. 3532
- Woolsey, S. E., & Weaver, T. A. 1986, *ARA&A*, 24, 205